Express Polymer Letters Vol.17, No.9 (2023) 900–912
Available online at www.expresspolymlett.com
https://doi.org/10.3144/expresspolymlett.2023.67

Research article

Spent coffee grounds utilization for green ultraviolet filter and nanocomposite fabrication

Ha Ngoc Giang[1*], *Chanh Cong Tran*[2], *Tuan Nguyen Anh Huynh*[2], *Phuong Thi Minh Doan*[1]

[1]Faculty of Chemical Technology, Ho Chi Minh City University of Industry and Trade, 140 Le Trong Tan Street, Tay Thanh Ward, Tan Phu District, Ho Chi Minh City, Viet Nam
[2]Faculty of Chemical and Food Technology, Ho Chi Minh City University of Technology and Education, 1 Vo Van Ngan Street, Linh Chieu Ward, Thu Duc City, Ho Chi Minh City, Viet Nam

Received 3 March 2023; accepted in revised form 12 May 2023

Abstract. Spent coffee grounds (SCGs), the main by-product in the coffee industry, were proposed as a starting material to fabricate both ultraviolet (UV) shielding material and nanocomposite based on polyvinyl alcohol (PVA). The extract using low SCGs concentration (0.25 wt%) contains a significant amount of UV-absorbing substances. The UV shielding film from 5 wt% PVA solution and SCGs extract (1 g SCGs/200 ml water) could shield most of the radiation in UV-B and UV-C regions and maintain 63% transmittance at 550 nm. The SCGs after washing were ball milled and the ultrasonic liquid processor was applied to synthesize SCGs nanoparticle. The effects of ultrasonic amplitude and hexadecyltrimethylammonium bromide (CTAB) on the particle's hydrodynamic diameter were investigated. The particle's size of 148 nm was obtained with 50% ultrasonic amplitude. Fourier-transformed infrared spectroscopy (FTIR) results confirmed the presence of hydroxyl groups (–OH) on the SCGs-based nanoparticle's surface. The tensile strength of PVA-SCGs nanocomposite was significantly improved. However, the presence of CTAB in the nano solution could not show a better tensile result. The organic compounds contained in the SCGs extract and even in the nano SCGs solution could enhance thermal oxidation stability for both UV shielding films and nanocomposites.

Keywords: *nanomaterials, polymer composites, reinforcements, spent coffee grounds, UV filter*

1. Introduction

Coffee has become one of the most popular beverages in many countries and massive waste including spent coffee grounds (SCGs) has been generated by the industry [1, 2]. Because of their low economic value, SCGs are often discarded as waste and it might affect human health and the environment [3]. The SCGs composition is highly varied because of different brewing methods and types of coffee. The main SCGs' components include carbohydrates, lignin, lipids, and protein [4–6]. Even after brewing, many bioactive phenolic compounds were found in SCGs [7–9]. These findings have made the popular waste material from the coffee industry become a potential source of natural antioxidant compounds. In a recent study, many products from SCGs could be utilized by extracting in water and hydrothermal liquefaction [10]. Many substances including polyphenol, polysaccharide, ketone, acid, ester *etc.* could be detected. Therefore, SCGs were considered as a bioresource that can be utilized for many applications. With high nutrient content, SCGs have been applied as a bio-fertilizer in agriculture [11, 12]. Properties of caffeine and other components from coffee could be applied in sunscreens [13–15] or solar cells [16]. Polyvinyl alcohol (PVA), a water-soluble polymer, was widely used in many applications because of its biocompatibility [17, 18]. Therefore, a

*Corresponding author, e-mail: hagn@hufi.edu.vn

combination of PVA and UV-absorbing substances in instant coffee had been proposed to form an environmentally friendly material that could shield lights in the UV region [19]. The fabricated films showed good transparency and thermal stability. The components of caffeine, chlorogenic acid, and melanoidin were assigned for the high performance of the PVA-based UV shielding films.

On the other hand, approximately 50 wt% of the SCGs were cellulose and hemicellulose [5]. Therefore, with the high demand for bio-degradable composite, many studies attempted to recycle SCGs as a bio-filler in plastic [20–22]. In the study by Catado *et al*. [23], the properties of pectin filled with SCGs were investigated to apply as food packaging materials. Although the hydrophobization and the reduction of water uptake were achieved, the mechanical properties were reduced with the addition of SCGs. SCGs also contain a significant amount of oil (more than 15%) [24, 25]. The oil extracted from SCGs could be utilized for bio-diesel production [26]. From another viewpoint, oil remaining in SCGs might affect the mechanical properties of the composite. SCGs after oil extraction could improve the mechanical and thermal properties of the formed composites [27, 28]. Leow *et al*. [29] also reported the enhancement in Young's modulus of epoxy resin by adding SCGs or oil-extracted SCGs. However, the tensile strength was significantly decreased because of poor interfacial compatibility between the hydrophilic SCGs-based fillers and the hydrophobic epoxy matrix. Although SCGs have been utilized as green fillers in many studies, less research reported nanomaterial from SCGs. In the nanotechnology field, the use of SCGs as a reducing agent to prepare silver or gold nanoparticles has been investigated [30–32]. In another study, lipid was removed from roasted coffee beans using *n*-hexane, and the components that remained in the solid residue were utilized to synthesize cellulose nanofibers (CNF) [33]. The coffee beans based-CNF was then applied to fabricate composites with PVA. Although the interaction of CNF and PVA had been discussed, the mechanical property of the composite was not reported. In other approaches, carbon dots could be synthesized from coffee bean shells [34] or SCGs [35]. Lee *et al*. [36] reported particles prepared directly from SCGs with the ability to improve the tensile strength of PVA-based composite. There was no oil-extraction step needed and the popular ball mill technique was applied to reduce the size of SCGs particles. However, the rather large average size of 240 nm and broad size distribution was obtained.

To the best of our knowledge, there is no report of the ability to fabricate stable SCGs nanoparticles under ultrasonic irradiation. Besides, the preparation of the SCGs particles included the washing steps to remove the water-soluble substances which might be still valuable in many cases. A simple approach and methodology to further utilize all SCGs components are still developing. In this study, green nanoparticles and nanocomposites based on SCGs formed with the assistance of an ultrasonic liquid processor shall be presented. Instead of instant coffee, the ability to reuse the extract from SCGs that were discarded during the washing step in the previous article [36] as green UV filters shall be confirmed and discussed.

2. Experimental section

2.1. Materials

PVA (hydrolysis degree: 85-90%, viscosity: 20.5–24.5 mPa·s) was purchased from Shanghai Aladdin Bio-Chem Technology Co. Ltd (China). Hexadecyltrimethylammonium bromide (CTAB) (≥98%) was the product of Sigma-Aldrich (Merck, USA). SCGs were collected from a local coffee shop. The caffeine standard was obtained from the Institute of Drug Quality Control – Ho Chi Minh City (IDQC-HCMC) (Viet Nam). The chlorogenic acid standard was supplied by Acros Organics (Thermo Scientific, United Kingdom).

2.2. Methods

The fabrication methods were summarized in Figure 1 which includes the preparation of UV shielding films and PVA-based nanocomposites.

Preparation of UV shielding films

The collected SCGs were washed with cold distilled water to remove dust and impurity. The product was dried in the oven (80 °C) for 24 h. The dried SCGs were weighed (x [g] from 0.1 to 30 g) and put into an Erlenmeyer flask containing 200 ml of double distilled water. The mixture was boiled and stirred for 10 min. Then, the obtained mixture was filtered, and the solution was placed into centrifuge tubes. The centrifugation at 5000 rpm for 10 min was applied. The aqueous SCGs extract was collected and directly used for the next step. PVA powder was weighed and added to the extract. For the UV shielding film fabrication,

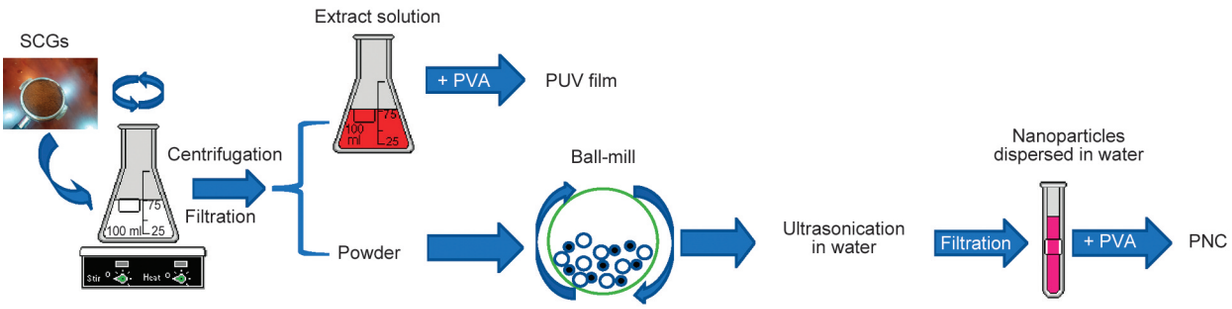

Figure 1. Fabrication scheme for UV shielding and nanocomposite samples.

the PVA concentration was fixed at 5 wt% which is similar to the previous report [19] for comparison. The mixture was stirred at room temperature until a clear, homogeneous solution was obtained. The polymeric solution was poured into a Teflon petri dish. The solvent was gradually evaporated at 40 °C to form PVA-based UV shielding (PUV) films. The samples were marked as PUV-*x*, where *x* is the mass [g] of SCGs used in 200 ml H_2O in the extraction step.

Preparation of nanoparticle solution and PVA-based nanocomposite

The remaining solid obtained after aqueous extraction from the above procedure was further washed with boiled distilled water until there was no change in the solution color. This step was conducted to remove water-soluble substances that remained in the extracted SCGs. The solid after washing was again dried in the oven (80 °C) for 24 h to obtain a dry powder. The powder was put into a cylindrical ceramic ball mill (speed: 225 rpm) for 40 min. Then, the fine powder was mixed with double distilled water (concentration: 1 wt%). The samples with CTAB were prepared in a similar method. Instead of water, the CTAB solutions (concentration: 60 or 250 mg/100 ml H_2O) were mixed with the ground SCGs before moving to the next step.

The mixtures in a 50 ml centrifuge tube were placed into an ultrasonic liquid processor (Net power output: 500 Watt, frequency: 20 kHz, vibra-Cell VC505, Sonics & Materials, Inc., USA). A standard probe equipped with a replaceable tip (diameter: 13 mm, amplitude set at 100%: 126 μm) was used. The preset sonication amplitude parameter varied at 30, 50, and 70%. The sonicated mixture was filtered using a qualitative filter paper (Grade 101, Pore size: 20–25 μm, Hangzhou Special Paper Industry Co., Ltd., China) or a glass fiber filter (GF/A, pore size: 1.6 μm, diameter: 47 mm, Whatman, United Kingdom) to obtain an aqueous solution contained nanoparticles. PVA was added into the SCGs nano-solutions to form homogenous mixtures with varied polymer concentrations (3, 5, 8, or 10 wt%). The PVA-nano SCGs solutions were dried in a silicone mold in ambient conditions to form PVA-based nanocomposite (PNC) films. The nanocomposite samples were named PNC-*y*, where *y* is the PVA concentration in the nano-solution.

2.3. Characterization

UV-Visible spectroscopy was applied to measure the absorbance of the SCGs extract and characterize the transmission of the PUV films. The spectra were obtained using a double-beam spectrophotometer (V730, Jasco, Japan). The scanning mode was applied, and the spectra were achieved in the wavelength region of 250 to 700 nm.

To determine the particle size, the dynamic light scattering (DLS) technique was applied using the equipment of Zetasizer Pro (Malvern, United Kingdom). The backscatter system (detector angle of 173°) and the measuring temperature of 25 °C were set. The sample was equilibrated for 60 s before conducting the measurement. The zeta potential values were determined using the same equipment with disposable folded capillary cells. Each sample was measured three times and an average value was calculated. In addition, a transmission electron microscope (TEM) (JEM 1010, JEOL, Japan) was also applied to directly observe the SCGs-based nanoparticles.

Fourier transform infrared (FTIR) measurement was conducted using the equipment of FTIR-8400s (Shimadzu, Japan). The samples were mixed with KBr powder (Nacalai Tesque, Kyoto, Japan) (approximately 0.1 wt%) and put into a stainless steel mold (diameter: 1.5 cm). The pressure was applied using a manual hydraulic press to form KBr pellets. The FTIR transmission mode was carried out from 4000 to 400 cm^{-1} wavenumber.

Thermogravimetric analyzer (TGA) (TGA 55, TA Instruments Co., USA) was performed from room temperature to 700 °C (heating rate: 10 °C·min^{-1}). To confirm the thermal oxidative stability of the samples, oxygen purge gas was applied (balance/sample flow rate: 40/25 ml/min).

Mechanical properties were evaluated using a tensile testing machine (FS3000, Testometric, United Kingdom). The experiment was conducted with similar conditions compared to the published research [36]. The film samples were cut into rectangular shapes (15×50 mm). Thickness was measured using a digital micrometer. The tensile test was carried out with a speed of 5 mm·min^{-1} to obtain the stress-strain curve. The maximum stress and elongation values in the curve were detected.

The homogeneity of the polymer nanocomposite was monitored using an optical microscope (B-293, Optika, Italy). The microscope was equipped with 10× and 40× objective lenses. The magnified images of the samples were captured by a CMOS camera and exported using Optika Proview software.

3. Results and discussion

Figure 2 showed the UV-Visible absorbance spectrum of the extract obtained from 0.5 g SCGs in 200 ml H_2O. As can be seen, the spectrum contained two main peaks at 278.8 and 322.8 nm. Compared to the pure substances (caffeine and chlorogenic acid) which are usually presented in coffee extract, the peak at 322.8 nm might be originally from chlorogenic acid. However, compared to caffeine's spectrum (peak is at 272.4 nm), the detected peak in the extract (278.8 nm) was slightly shifted to a higher wavelength region. This phenomenon might be due to the interference of the other UV-absorbing substances (chlorogenic acid and melanoidin) in the extract [37, 38]. The UV-Visible absorbance spectrum of the SCGs extract was identical to the reported result using instant coffee [19]. In Figure 2 results, although the extraction was conducted with approximately 0.25 wt% SCGs aqueous mixture for only 10 min, the absorbance values of all detected peaks were higher than 1. Therefore, it could be concluded that the extract from SCGs might contain a significant amount of similar organic compounds presented in the instant coffee solution. It is worth noting that the extraction procedure is rather simple, and the process is similar to the washing step in the previous study [36]. It might open a new approach to utilizing the waste product which is cheaper than the original instant coffee. In the next experiment, the SCGs extract was mixed with PVA to confirm the UV-shielding capability of the formed films.

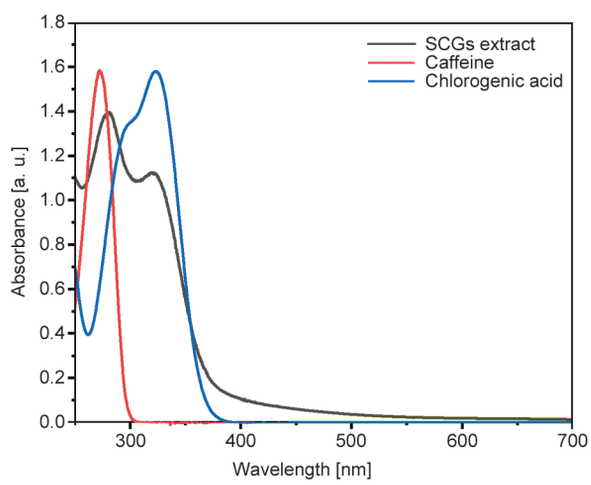

Figure 2. UV-Visible absorption spectra (250 to 700 nm) of SCGs extract (0.5 g/200 ml H_2O), caffeine, and chlorogenic acid solution (30 ppm).

The transmittance values and the images of PVA films mixed with different types of SCGs extracts were summarized in Figure 3. The UV-shielding ability of the film samples might be affected by the thickness of the film sample. Therefore, the values of transmittance divided by the corresponding thicknesses (in micrometer) were also shown in Figure 3b. However, the relative positions of the spectra obtained in Figure 3b are similar to that in Figure 3a. As can be observed, pure PVA film provides the highest transparency. However, PVA also had the worse protection in the region of UV-A, B, and C (the wavelength is less than 400 nm). When the amount of SCGs used for aqueous solution extraction was 5, 10, 20, or 30 g/200 ml H_2O, the UV region might be completely cut off after passing the PVA-based films. The transparency in the visible region was also reduced accordingly. On the other hand, when only 0.1 or 0.5 g SCGs was used, the transmittance values at the visible wavelengths were improved. However, there was part of UV light that might be allowed to pass through the films. The sample prepared with only 1 g SCGs provided a reasonable transmittance for the visible lights. The transmittance measured at 550 nm is 63% while this value is 84% for the pure PVA film. Few wavelengths in the UV-A region remained slightly transparent. However, more damaging UV radiation from 290 to 350 nm could be mostly shielded. The investigation showed that the extracted solution

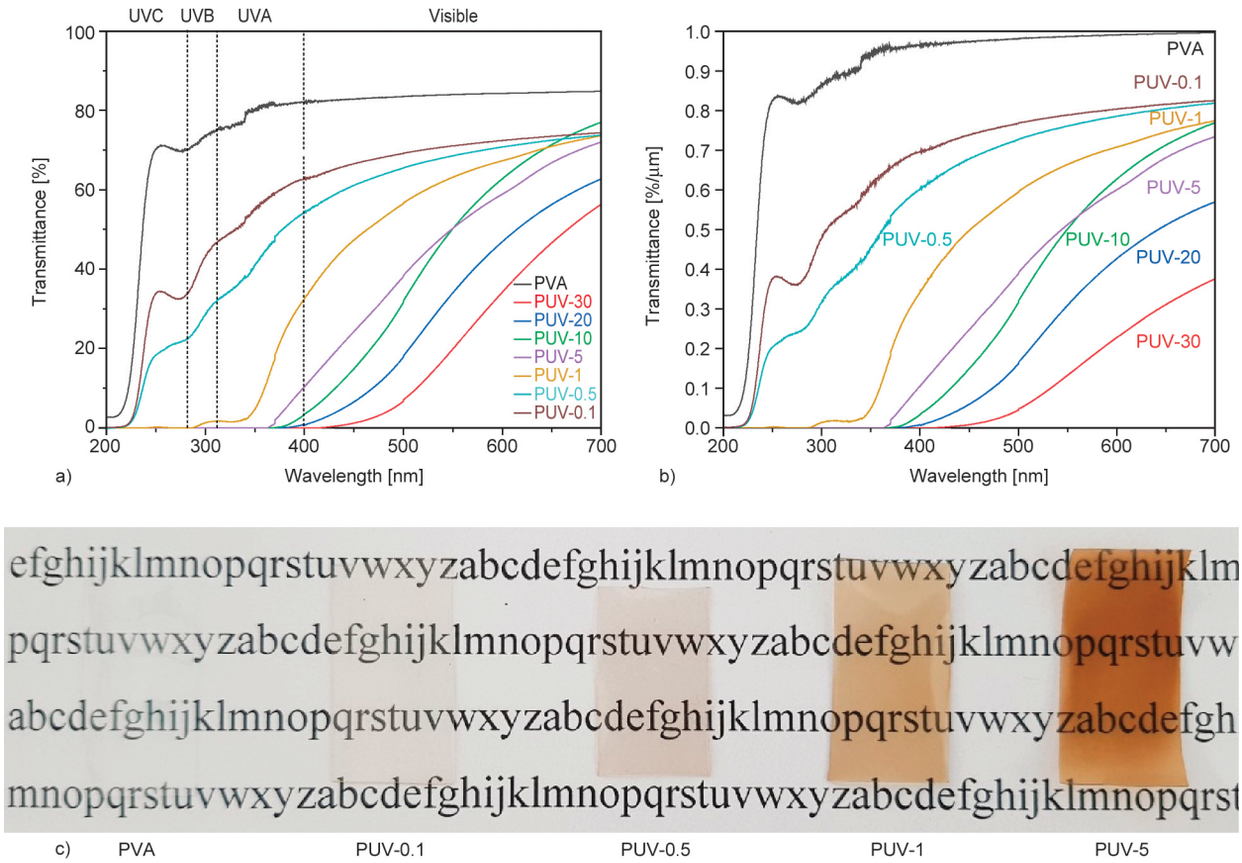

Figure 3. a) UV-Visible spectra, b) transmittance values/film's thicknesses spectra, and c) images of PVA film and PVA-based films mixed with various SCGs extractions.

obtained from only 1 g SCGs/200 ml H_2O (0.5 wt%) could provide a similar UV-shielding effect to the use of 1 wt% of instant coffee reported by the other group [19].

The SCGs after aqueous extraction was further utilized to synthesize nano-fillers. The washed SCGs were ball-milled before forming nanoparticles under the ultrasonic force in an aqueous solution. Ultrasonic amplitude was varied, and the DLS particle size results of the obtained nanoparticle were summarized in Figure 4 and Table 1. In this investigation, although the conventional filter paper was applied in the filtration step, the average particle size of less than 300 nm still could be achieved. As can be seen, when the amplitude was increased, the smaller Z-average values might be obtained (Table 1). In all cases, although

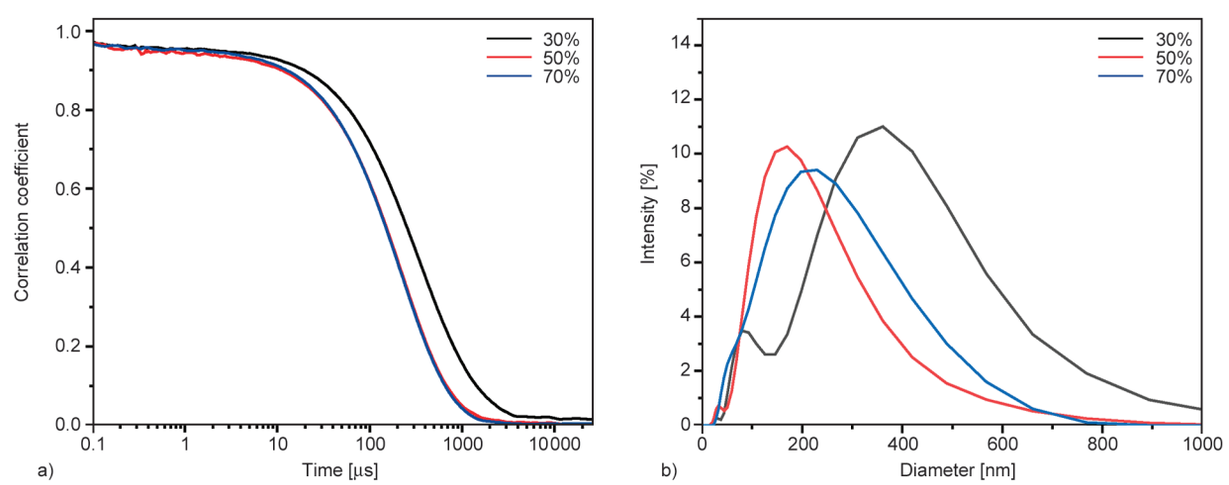

Figure 4. a) Plots of the correlation coefficient as a function of time and b) intensity size distribution spectra of SCGs nanoparticle solutions fabricated using qualitative filter papers and various ultrasonic amplitudes.

Table 1. DLS results of SCGs nanoparticle solutions using qualitative filter papers and various ultrasonic amplitudes.

Amplitude [%]	30	50	70
Z-Average [nm]	242.6±12.5	154.3±1.0	152.3±0.9
Polydispersity index, PI	0.532±0.071	0.333±0.028	0.291±0.002
Peak mean (Intensity distribution) [nm]	386.9±91.7	171.2±25.8	208.3±18.6

the polydispersity index (PI) values were not large, there were other small peaks that appeared in the DLS intensity distribution which indicated two types of the particle system. It is worth noting that the SCGs components after washing might be mainly carbohydrates. Cellulose, hemicellulose, and lignin which are varied in molecular weight in SCGs might be the main reason for the polydispersity of the nano solutions. The amplitude represents the distance of the ultrasonic tip vibrating from the equilibrium position. Because the SCGs concentration dispersed in water was fixed, the increase in amplitude was directly proportional to the ultrasonic energy used to break down the milled SCGs into smaller particles. Therefore, there was a significant difference between the results obtained from 30 and 50% amplitude. The size distribution was also shifted to a smaller size region. When the amplitude was up to 70%, although the intensity signal of the smaller particle system was slightly increased, the distribution was also stretched to the larger particle area. However, the autocorrelation curves and Z-average values were nearly unchanged. In addition, the solution temperature quickly increased, and it is difficult to control. Therefore, the amplitude of 50% was applied for the next investigation.

Instead of the qualitative filter paper, the glass fiber filter with a smaller pore size was used to confirm the ability to further reduce the particle size. The DLS results were shown in Table 2. As can be seen, the particle size was slightly improved by applying the glass fiber filter. Figure 5 showed the TEM images of the SCGs particles prepared without using CTAB. As can be seen, this is another evidence that the nanoparticles could be successfully fabricated from SCGs with the assistance of ultrasonication. Although small particles (<100 nm) could be observed, many large particles and aggregations were also detected. The TEM images were in agreement with the polydispersed distribution obtained in the DLS results. Because of the ability to stabilize the nanoparticle, CTAB has been widely applied in nanomaterials research [39–41]. Therefore, in this study, the nanoparticle formed under the presence of CTAB was investigated and the size values were also

Table 2. DLS results of SCGs nanoparticle solutions using glass fiber filters and various CTAB concentrations.

CTAB [mg/100 ml]	0	60	250
Z-average [nm]	148.4±0.7	308.9±3.0	190.7±3.5
Polydispersity index, PI	0.214±0.002	0.308±0.008	0.255±0.016
Peak mean (Intensity distribution) [nm]	179.1±15.9	480.8±158.7	208.3±18.6

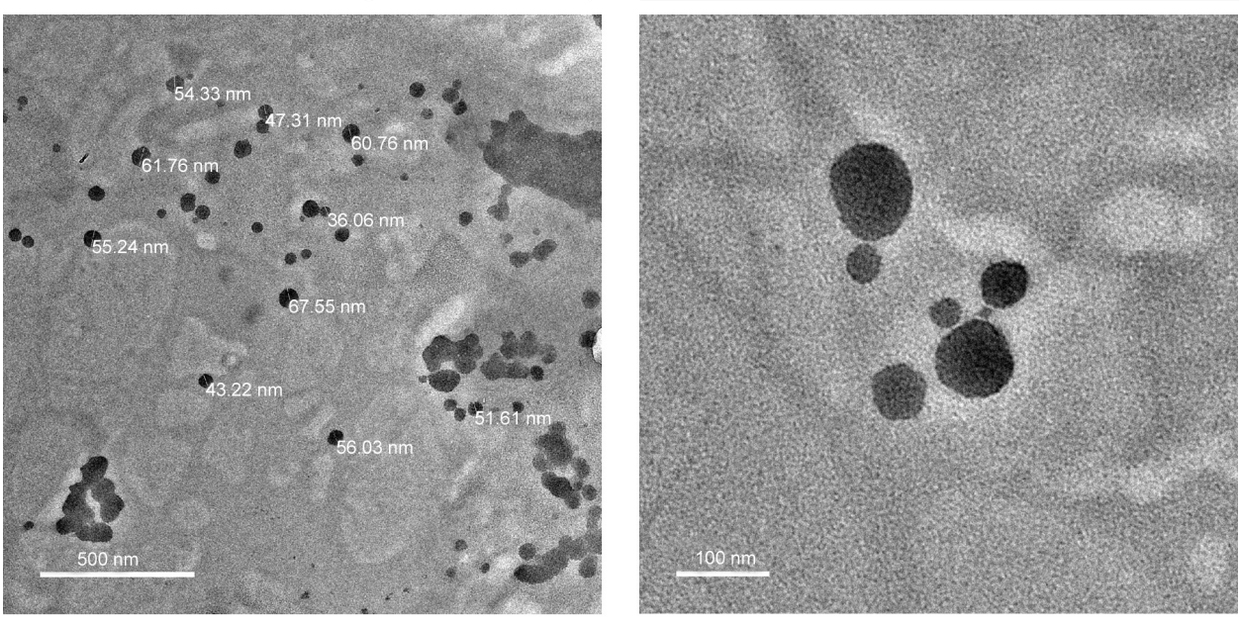

a) b)

Figure 5. TEM images of SCGs-based nanoparticle sample without CTAB at a magnification of a) 10 000× and b) 30 000×.

shown in Table 2. The larger particle size was obtained with 60 mg/100 ml CTAB. By increasing to 250 mg/100 ml, although the particle size could be reduced to 190 nm, the result still is higher than that of the sample formed without CTAB (148 nm). This phenomenon might be due to the capping effect of CTAB on the formed nanoparticles [42]. The CTAB structure contains a hydrophilic headgroup (quaternary amine) and a hydrophobic tail (alkyl chain). The SCGs-based nanoparticle with the hydrophilic surface could be covered by CTAB molecules via the charged headgroups. The second layer might be formed by the interaction of hydrophobic alkyl chains among the CTAB molecules. As a result, the CTAB bilayer left the positive headgroups exposed to the solution. Therefore, the hydrodynamic diameter detected by the DLS technique might be increased. This explanation was reconfirmed by considering the particle surface's charge. The zeta potential was –17.7±1.6 mV while this value was positive (25.3±0.4 mV) by adding CTAB to the solution. The average particle size obtained by applying the current protocol is significantly smaller than the previous report (240 nm) [36]. Without removing the solvent, the nanoparticles dispersed in water were directly used for the next steps of nanocomposite fabrication to limit the ability of aggregation.

The nanoparticles prepared using glass filter paper were added into the PVA matrix to confirm the ability to improve the mechanical properties. The tensile results for the samples fabricated from the nano solution with and without CTAB (250 mg/100 ml H_2O) were shown in Figure 6. Firstly, the film samples were fabricated using 5 and 3 wt% of PVA (PNC-5 or 3 and PNC-5-CTAB or 3-CTAB) and the tensile results were compared. As can be seen, when the SCGs particles prepared with CTAB were mixed with PVA, the tendency of reducing tensile strength (TS) was obtained. The mechanical enhancement could not be observed in all samples with the presence of CTAB. The component of SCGs might contain fatty acids which are difficult to remove during the washing step with pure water. However, these components might leak to the formed nano solution

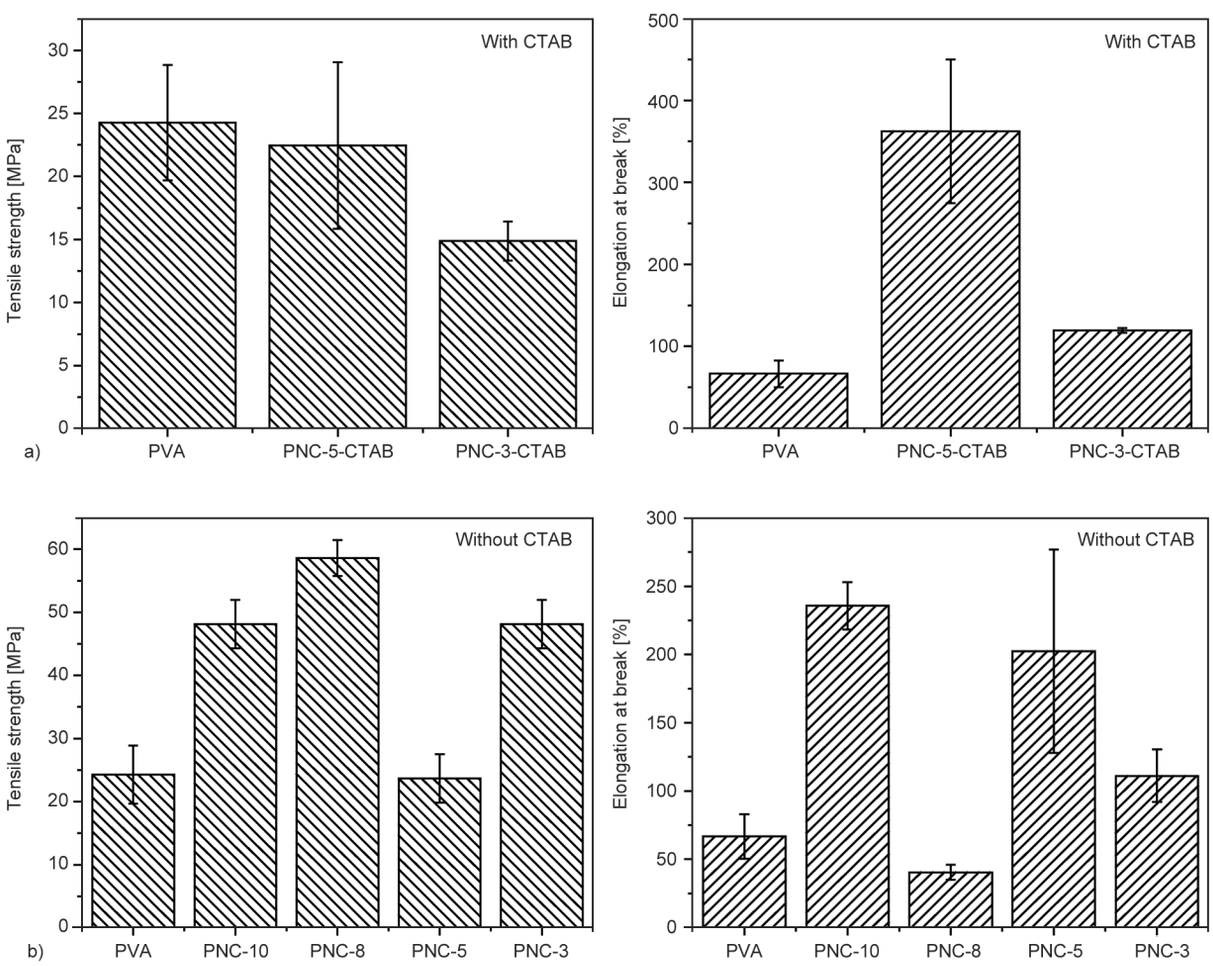

Figure 6. Tensile result for PVA-based nanocomposites from SCGs: a) with CTAB; b) without CTAB.

with the presence of a surface-active reagent of CTAB. These long alkyl chain components might act as a plasticizer in the PVA matrix and reduce the mechanical properties. In addition, the nanoparticles covered by CTAB molecules might not be compatible with the PVA matrix. Therefore, the study was focused on the samples without using CTAB. On the other hand, when SCGs nanoparticles prepared without CTAB were added, TS was significantly improved. The highest TS value (~58 MPa) achieved with 8 wt% of PVA (PNC-8) was more than two times higher than that of the original PVA film (~24 MPa). The same SCGs nano solution was used in all cases while the PVA concentration was decreased. After evaporating water to form nanocomposite, the film samples with less PVA had a higher nanoparticle concentration. When the PVA concentration was 5 wt%, the number of SCGs nanoparticles contained in the composite was high enough to cause some aggregation (Figure 7c). This might be the main reason for the reduction of the mechanical properties. Although the sample of PNC-3 still showed a high TS value, the aggregation of nanoparticles because of high concentration could not be ensured as can be observed in Figure 7d. In addition, the TS value could not be further improved compared to the PNC-8 sample. A smaller nanoparticle concentration with higher mechanical properties was preferred. Interestingly, the PNC-10 sample with the smallest amount of nanoparticles showed an improvement in both TS and elongation at break values.

The effect of SCGs nanoparticles on the stress-strain curves was shown in Figure 8. All samples showed the first linear increase of stress followed by yielding and plastic deformation. Compared to PVA, the elastic region was significantly expanded to a higher stress region in the samples with nanoparticles addition (except the PNC-5 sample). These samples also performed a slight decrease of stress after yielding which is the typical necking in the tensile test. This phenomenon is because of the formation of localized domains in which the polymer chains were re-oriented to a fibrous structure. The nanoparticle occupied in the spaces between the polymer chains might assist the unfolding process. Therefore, the PNC-10 sample with a low nanoparticle concentration could possess good performance in both TS and elongation properties. However, in the PNC-8 with more nano-SCGs, the interaction of filler and polymer chains was dominated. As a result, the increase of TS and decrease of elongation were obtained. To further confirm the compatibility of PVA molecules and SCGs nanoparticles, FTIR measurement was performed, and the results were summarized in Figure 9. The nanoparticle was prepared via two steps of mechanical treatment including ball milling and ultrasonic radiation. The FTIR spectra shown in Figure 9a could reveal the changing of functional groups with each step. The obtained results of SCGs were similar to the previous publication [29]. The peaks at 2923 and 2853 cm^{-1} assigned as asymmetric and symmetric C–H vibrations appeared in all SCGs samples. The peak at 1745 cm^{-1} belonging to C=O bond stretching was also detected in all types of SCGs. The C=O signal might come from various antioxidant substances contained in the SCGs such as caffeine, chlorogenic acid, or fatty acids. Although the signal of this functional group became weaker in the nanoparticle FTIR spectrum, the existence of C=O might still indicate a small amount of the bio-active components remained. In the 4000–3200 cm^{-1} region, peaks could not be detected clearly in the SCGs after washing with boiled water. However, some small peaks in this region belonging to O–H or N–H bond stretching appeared in the SCGs sample after the ball milling process. This result indicated that the washing process had removed most of the water-soluble substances from the SCGs' surface. However, after milling, the raw SCGs were broken down into smaller pieces and these functional groups trapped inside might be again detectable. Interestingly, the nanoparticle showed a large peak at 3429 cm^{-1}. In this study, water was used as a dispersed environment and only particles with the polar groups can be stabilized in the medium. Therefore, SCGs-based nanoparticle surfaces might be covered by –OH groups. This might be one of the advantages of the current fabrication method. Because of the presence of polar groups, the synthesized nanoparticle might be dispersed better in the matrix of PVA which also possesses many hydroxyl groups in the side chain. Figure 9b showed the spectrum of PVA in which the FTIR peaks were also detected at similar wavenumbers compared to the previous study [43]. As can be observed, the PNC-8 sample's FTIR spectrum contained the main peaks originating from its components. However, in the case of the nanocomposite, the large peak that appeared in the 4000–3200 region was shifted to a lower wavenumber comparing the similar peaks of nanoparticle and PVA. This phenomenon might be

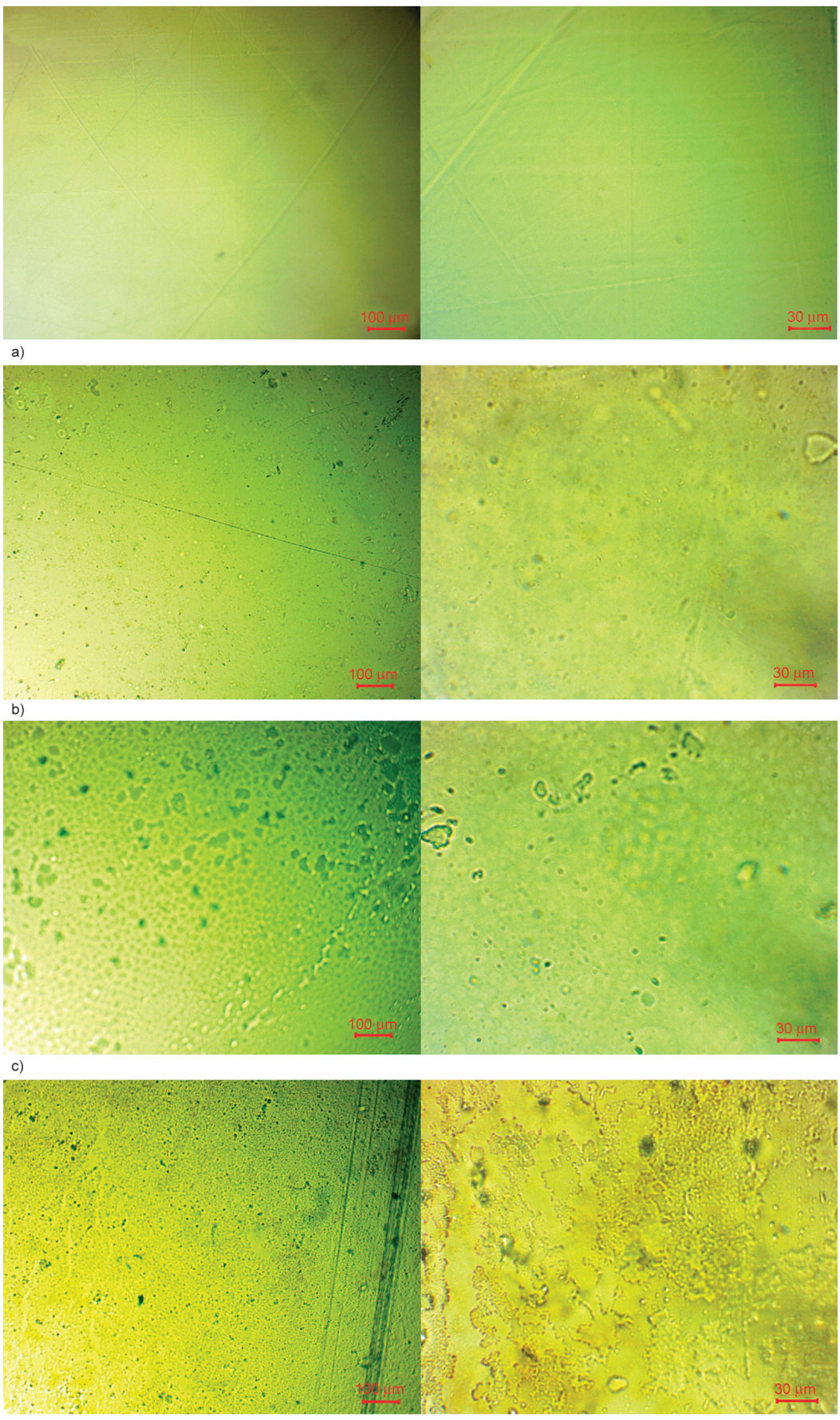

Figure 7. Optical microscope images of PNC at 10× and 40× objective lenses: a) PNC-10, b) PNC-8, c) PNC-5, and d) PNC-3.

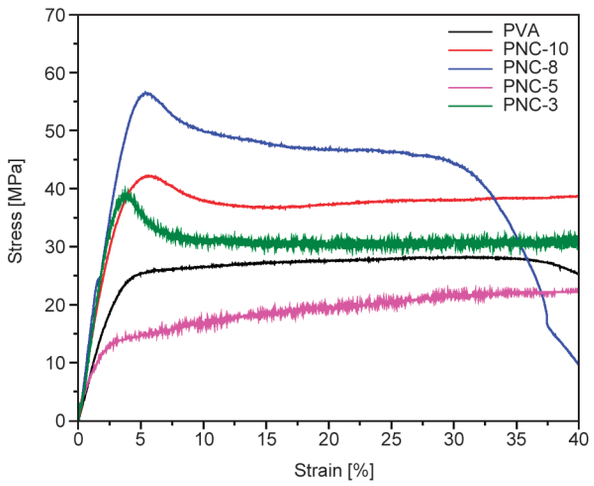

Figure 8. Stress-strain curve of PVA-based nanocomposite with SCGs.

an indicator of good compatibility between the nanofiller and the matrix.

Thermal properties in the oxygen atmosphere could reveal the capability against oxidative degradation of the fabricated film samples. The TGA results were summarized in Figure 10. As can be observed, the first loss of weight occurred continuously from room temperature until reaching 150 °C was assigned to the evaporation of water that remained in the film samples. The main and significant weight loss was activated when the temperature reached 200 °C. This large decrease in the TGA signal was because of thermal degradation and decomposition of PVA and organic substances in the matrix. Three types of samples (PVA, PUV, and PNC) showed similar TGA transitions. To remove the interference of water desorption signals, the TGA data were normalized with a value at 170 °C, and the results were shown in Figure 10b. As can be seen, although the difference is small, the PUV sample still clearly showed a better

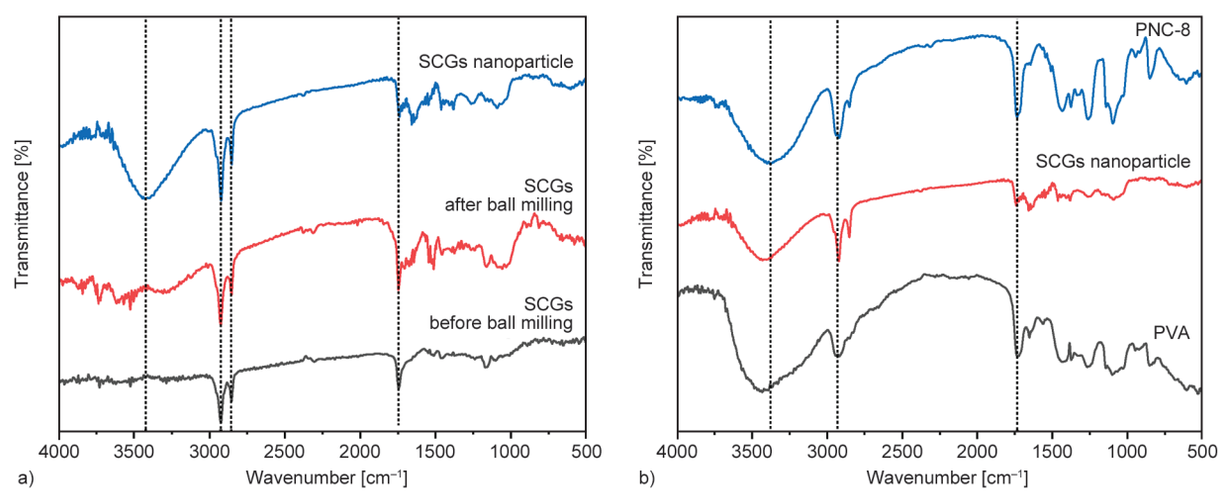

Figure 9. FTIR spectra of a) SCGs samples before and after the mechanical treatments; b) PNC-8 sample in comparison to SCGs nanoparticle and PVA.

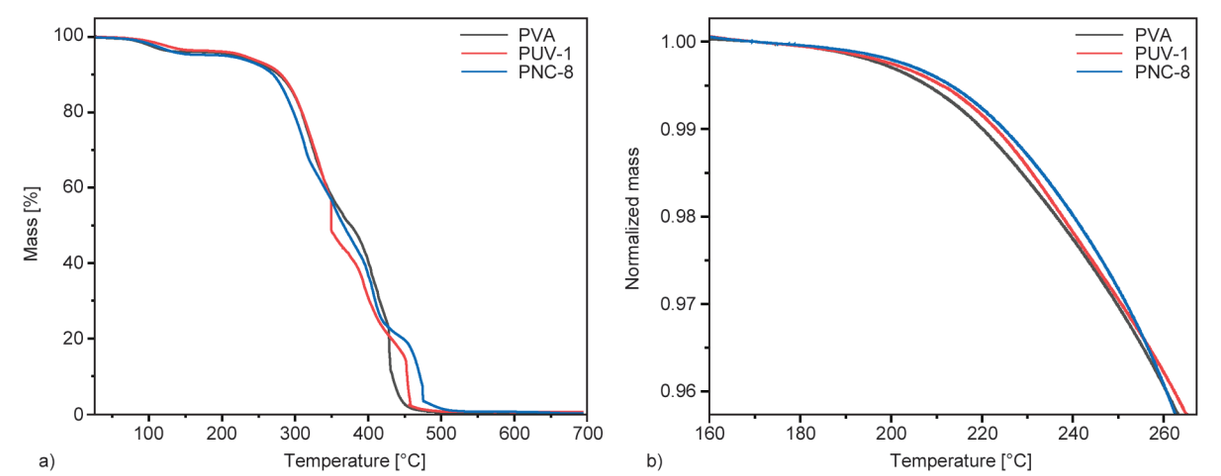

Figure 10. TGA results for PVA, PUV-1, and PNC-8: a) plotted from room temperature to 700 °C; b) plotted as normalized value with weight loss at 170 °C from 160 to 265 °C.

thermal-oxidative degradation. This result is in agreement with the previous report [19]. Interestingly, the weight loss signal for the PNC sample also occurred more slowly than that of the original PVA. The nanoparticle prepared in this current study might contain not only carbohydrate particles but also some amount of antioxidant remaining (caffein or chlorogenic acid). Therefore, the PVA-based composite reinforced by the nanofiller from SCGs could possess both strong mechanical properties and resistance to thermal-oxidative degradation.

4. Conclusions

A green approach of the utilization of both extract solution and the remaining carbohydrate from SCGs respectively for UV filters and nanofillers was confirmed. Although a low concentration of SCGs (~0.25 wt%) was extracted in boiled water for a short time (10 min), the extract contained a significant amount of UV-absorbing substances such as caffeine, chlorogenic acid, and melanoidin. UV shielding materials could be fabricated successfully from 5 wt% PVA solution and the SCGs extracts. The PUV-1 showed complete shielding in the UV-C and most of the UV-B regions while the 63% transparency at 550 nm was maintained. By applying 50% ultrasonic amplitude and filtrating through glass fiber filters, the nano-SCGs solution with an average particle diameter of 148 nm could be obtained. A new and strong FTIR peak that appeared at 3429 cm^{-1} could confirm the existence of the OH groups on the surface of nanoparticles. Owing to the strong interaction between the polar groups, the compatibility between the PVA matrix and nano SCGs fillers could be improved. TS value of the nanocomposite fabricated from PVA and nano SCGs particles was significantly higher (more than two times) than that of the original PVA film. The addition of CTAB could change the value of zeta potential from minus to positive value. However, the samples fabricated with CTAB could not yield a better result in nanoparticle size and nanocomposite's mechanical properties. The presence of antioxidant compounds remaining in the nano solution might be the main reason for the enhancement in thermal oxidative properties for both PVA-based UV shielding material and nanocomposite.

Acknowledgements

The authors would like to thank MSc Le Thi Kim Anh and MSc Truong Thi Phuong Dung for providing laboratory assistant services.

References

[1] Murthy P. S., Madhava Naidu M.: Sustainable management of coffee industry by-products and value addition – A review. Resources, Conservation and Recycling, **66**, 45–58 (2012). https://doi.org/10.1016/j.resconrec.2012.06.005

[2] Esquivel P., Jiménez V. M.: Functional properties of coffee and coffee by-products. Food Research International, **46**, 488–495 (2012). https://doi.org/10.1016/j.foodres.2011.05.028

[3] Fernandes A. S., Mello F. V. C., Thode Filho S., Carpes R. M., Honório J. G., Marques M. R. C., Felzenszwalb I., Ferraz E. R. A.: Impacts of discarded coffee waste on human and environmental health. Ecotoxicology and Environmental Safety, **141**, 30–36 (2017). https://doi.org/10.1016/j.ecoenv.2017.03.011

[4] Kovalcik A., Obruca S., Marova I.: Valorization of spent coffee grounds: A review. Food and Bioproducts Processing, **110**, 104–119 (2018). https://doi.org/10.1016/j.fbp.2018.05.002

[5] Ballesteros L. F., Teixeira J. A., Mussatto S. I.: Chemical, functional, and structural properties of spent coffee grounds and coffee silverskin. Food and Bioprocess Technology, **7**, 3493–3503 (2014). https://doi.org/10.1007/s11947-014-1349-z

[6] McNutt J., He Q.: Spent coffee grounds: A review on current utilization. Journal of Industrial and Engineering Chemistry, **71**, 78–88 (2019). https://doi.org/10.1016/j.jiec.2018.11.054

[7] Zuorro A., Lavecchia R.: Spent coffee grounds as a valuable source of phenolic compounds and bioenergy. Journal of Cleaner Production, **34**, 49–56 (2012). https://doi.org/10.1016/j.jclepro.2011.12.003

[8] Pavlović M. D., Buntić A. V., Šiler-Marinković S. S., Dimitrijević-Branković S. I.: Ethanol influenced fast microwave-assisted extraction for natural antioxidants obtaining from spent filter coffee. Separation and Purification Technology, **118**, 503–510 (2013). https://doi.org/10.1016/j.seppur.2013.07.035

[9] Panusa A., Zuorro A., Lavecchia R., Marrosu G., Petrucci R.: Recovery of natural antioxidants from spent coffee grounds. Journal of Agricultural and Food Chemistry, **61**, 4162–4168 (2013). https://doi.org/10.1021/jf4005719

[10] Zhang S., Yang J., Wang S., Rupasinghe H. P. V., He Q.: Experimental exploration of processes for deriving multiple products from spent coffee grounds. Food and Bioproducts Processing, **128**, 21–29 (2021). https://doi.org/10.1016/j.fbp.2021.04.012

[11] Ciesielczuk T., Rosik-Dulewska C., Poluszyńska J., Miłek D., Szewczyk A., Sławińska I.: Acute toxicity of experimental fertilizers made of spent coffee grounds. Waste and Biomass Valorization, **9**, 2157–2164 (2018). https://doi.org/10.1007/s12649-017-9980-3

[12] Cervera-Mata A., Navarro-Alarcón M., Delgado G., Pastoriza S., Montilla-Gómez J., Llopis J., Sánchez-González C., Rufián-Henares J. Á.: Spent coffee grounds improve the nutritional value in elements of lettuce (*Lactuca sativa* L.) and are an ecological alternative to inorganic fertilizers. Food Chemistry, **282**, 1–8 (2019). https://doi.org/10.1016/j.foodchem.2018.12.101

[13] Rosado C., Tokunaga V. K., Sauce R., de Oliveira C. A., Sarruf F. D., Parise-Filho R., Maurício E., de Almeida T. S., Velasco M. V. R., Baby A. R.: Another reason for using caffeine in dermocosmetics: Sunscreen adjuvant. Frontiers in Physiology, **10**, 519 (2019). https://doi.org/10.3389/fphys.2019.00519

[14] Lu Y-P., Lou Y-R., Xie J-G., Peng Q-Y., Zhou S., Lin Y., Shih W. J., Conney A. H.: Caffeine and caffeine sodium benzoate have a sunscreen effect, enhance UVB-induced apoptosis, and inhibit UVB-induced skin carcinogenesis in Skh-1 mice. Carcinogenesis, **28**, 199–206 (2007). https://doi.org/10.1093/carcin/bgl112

[15] Marto J., Gouveia L. F., Chiari B. G., Paiva A., Isaac V., Pinto P., Simões P., Almeida A. J., Ribeiro H. M.: The green generation of sunscreens: Using coffee industrial sub-products. Industrial Crops and Products, **80**, 93–100 (2016). https://doi.org/10.1016/j.indcrop.2015.11.033

[16] Hu X., Huang H., Hu Y., Lu X., Qin Y.: Novel bio-based composite phase change materials with reduced graphene oxide-functionalized spent coffee grounds for efficient solar-to-thermal energy storage. Solar Energy Materials and Solar Cells, **219**, 110790 (2021). https://doi.org/10.1016/j.solmat.2020.110790

[17] Kumar A., Han S. S.: PVA-based hydrogels for tissue engineering: A review. International Journal of Polymeric Materials and Polymeric Biomaterials, **66**, 159–182 (2017). https://doi.org/10.1080/00914037.2016.1190930

[18] Kamoun E. A., Kenawy E-R. S., Chen X.: A review on polymeric hydrogel membranes for wound dressing applications: PVA-based hydrogel dressings. Journal of Advanced Research, **8**, 217–233 (2017). https://doi.org/10.1016/j.jare.2017.01.005

[19] Lyu Y., Gu X., Mao Y.: Green composite of instant coffee and poly(vinyl alcohol): An excellent transparent UV-shielding material with superior thermal-oxidative stability. Industrial and Engineering Chemistry Research, **59**, 8640–8648 (2020). https://doi.org/10.1021/acs.iecr.0c00413

[20] Gaidukova G., Platnieks O., Aunins A., Barkane A., Ingrao C., Gaidukovs S.: Spent coffee waste as a renewable source for the production of sustainable poly (butylene succinate) biocomposites from a circular economy perspective. RSC Advances, **11**, 18580–18589 (2021). https://doi.org/10.1039/D1RA03203H

[21] García-García D., Carbonell A., Samper M. D., García-Sanoguera D., Balart R.: Green composites based on polypropylene matrix and hydrophobized spend coffee ground (SCG) powder. Composites Part B: Engineering, **78**, 256–265 (2015). https://doi.org/10.1016/j.compositesb.2015.03.080

[22] Wu C-S.: Renewable resource-based green composites of surface-treated spent coffee grounds and polylactide: Characterisation and biodegradability. Polymer Degradation and Stability, **121**, 51–59 (2015). https://doi.org/10.1016/j.polymdegradstab.2015.08.011

[23] Cataldo V. A., Cavallaro G., Lazzara G., Milioto S., Parisi F.: Coffee grounds as filler for pectin: Green composites with competitive performances dependent on the UV irradiation. Carbohydrate Polymers, **170**, 198–205 (2017). https://doi.org/10.1016/j.carbpol.2017.04.092

[24] Al-Hamamre Z., Foerster S., Hartmann F., Kröger M., Kaltschmitt M.: Oil extracted from spent coffee grounds as a renewable source for fatty acid methyl ester manufacturing. Fuel, **96**, 70–76 (2012). https://doi.org/10.1016/j.fuel.2012.01.023

[25] de Melo M. M. R., Barbosa H. M. A., Passos C. P., Silva C. M.: Supercritical fluid extraction of spent coffee grounds: Measurement of extraction curves, oil characterization and economic analysis. The Journal of Supercritical Fluids, **86**, 150–159 (2014). https://doi.org/10.1016/j.supflu.2013.12.016

[26] Efthymiopoulos I., Hellier P., Ladommatos N., Kay A., Mills-Lamptey B.: Effect of solvent extraction parameters on the recovery of oil from spent coffee grounds for biofuel production. Waste and Biomass Valorization, **10**, 253–264 (2019). https://doi.org/10.1007/s12649-017-0061-4

[27] Tellers J., Willems P., Tjeerdsma B., Sbirrazzuoli N., Guigo N.: Spent coffee grounds as property enhancing filler in a wholly bio-based epoxy resin. Macromolecular Materials and Engineering, **306**, 2100323 (2021). https://doi.org/10.1002/mame.202100323

[28] Wu H., Hu W., Zhang Y., Huang L., Zhang J., Tan S., Cai X., Liao X.: Effect of oil extraction on properties of spent coffee ground–plastic composites. Journal of Materials Science, **51**, 10205–10214 (2016). https://doi.org/10.1007/s10853-016-0248-2

[29] Leow Y., Yew P. Y. M., Chee P. L., Loh X. J., Kai D.: Recycling of spent coffee grounds for useful extracts and green composites. RSC Advances, **11**, 2682–2692 (2021). https://doi.org/10.1039/D0RA09379C

[30] Chien H-W., Kuo C-J., Kao L-H., Lin G-Y., Chen P-Y.: Polysaccharidic spent coffee grounds for silver nanoparticle immobilization as a green and highly efficient biocide. International Journal of Biological Macromolecules, **140**, 168–176 (2019). https://doi.org/10.1016/j.ijbiomac.2019.08.131

[31] Yust B. G., Rao N. Z., Schwarzmann E. T., Peoples M. H.: Quantification of spent coffee ground extracts by roast and brew method, and their utility in a green synthesis of gold and silver nanoparticles. Molecules, **27**, 5124 (2022). https://doi.org/10.3390/molecules27165124

[32] Zuorro A., Iannone A., Miglietta S., Lavecchia R.: Green synthesis of silver nanoparticles using spent coffee ground extracts: Process modelling and optimization. Nanomaterials, **12**, 2597 (2022). https://doi.org/10.3390/nano12152597

[33] Kanai N., Honda T., Yoshihara N., Oyama T., Naito A., Ueda K., Kawamura I.: Structural characterization of cellulose nanofibers isolated from spent coffee grounds and their composite films with poly(vinyl alcohol): A new non-wood source. Cellulose, **27**, 5017–5028 (2020). https://doi.org/10.1007/s10570-020-03113-w

[34] Zhang X., Wang H., Ma C., Niu N., Chen Z., Liu S., Li J., Li S.: Seeking value from biomass materials: Preparation of coffee bean shell-derived fluorescent carbon dots via molecular aggregation for antioxidation and bioimaging applications. Materials Chemistry Frontiers, **2**, 1269–1275 (2018). https://doi.org/10.1039/C8QM00030A

[35] Crista D. M. A., el Mragui A., Algarra M., da Silva J. C. G. E., Luque R., da Silva L. P.: Turning spent coffee grounds into sustainable precursors for the fabrication of carbon dots. Nanomaterials, **10**, 1209 (2020). https://doi.org/10.3390/nano10061209

[36] Lee H. K., Park Y. G., Jeong T., Song Y. S.: Green nanocomposites filled with spent coffee grounds. Journal of Applied Polymer Science, **132**, 42043 (2015). https://doi.org/10.1002/app.42043

[37] Rufián-Henares J. A., Pastoriza S.: Melanoidins in coffee. in 'Coffee in health and disease prevention' (ed.: Preedy V. R.) Academic Press, San Diego, 183–188 (2015).

[38] Belay A., Ture K., Redi M., Asfaw A.: Measurement of caffeine in coffee beans with UV/vis spectrometer. Food Chemistry, **108**, 310–315 (2008). https://doi.org/10.1016/j.foodchem.2007.10.024

[39] Singh Z., Singh I.: CTAB surfactant assisted and high pH nano-formulations of cuo nanoparticles pose greater cytotoxic and genotoxic effects. Scientific Reports, **9**, 5880 (2019). https://doi.org/10.1038/s41598-019-42419-z

[40] Elfeky S. A., Mahmoud S. E., Youssef A. F.: Applications of CTAB modified magnetic nanoparticles for removal of chromium (VI) from contaminated water. Journal of Advanced Research, **8**, 435–443 (2017). https://doi.org/10.1016/j.jare.2017.06.002

[41] Wei M-Z., Deng T-S., Zhang Q., Cheng Z., Li S.: Seed-mediated synthesis of gold nanorods at low concentrations of CTAB. ACS Omega, **6**, 9188–9195 (2021). https://doi.org/10.1021/acsomega.1c00510

[42] Sui Z. M., Chen X., Wang L. Y., Xu L. M., Zhuang W. C., Chai Y. C., Yang C. J.: Capping effect of CTAB on positively charged Ag nanoparticles. Physica E: Low-dimensional Systems and Nanostructures, **33**, 308–314 (2006). https://doi.org/10.1016/j.physe.2006.03.151

[43] Mansur H. S., Sadahira C. M., Souza A. N., Mansur A. A. P.: FTIR spectroscopy characterization of poly(vinyl alcohol) hydrogel with different hydrolysis degree and chemically crosslinked with glutaraldehyde. Materials Science and Engineering: C, **28**, 539–548 (2008). https://doi.org/10.1016/j.msec.2007.10.088